Observation of molecular-beam magnetic resonance of Li_3 clusters

Naoshi Hishinuma
Institute of Physics, College of Arts and Sciences, University of Tokyo, Komaba 3-8-1, Meguro-ku, Tokyo 153, Japan
(Received 22 June 1992)

The electron-spin-resonance spectrum was measured for pseudorotating $^6Li_3$ clusters by a matrix-free method, the molecular-beam magnetic resonance. Magnetic focusing was used for polarization and separation of the trimer beam. The spectrum indicates three equivalent lithium nuclei and gives the (average) isotropic spin population of $\bar{\rho}=0.231$ and a g factor of $g=2.002\,36$. The $\bar{\rho}$ value is very close to previous results obtained for matrix-isolated clusters, and the g factor is nearly equal to the free-electron value.

PACS number(s): 36.40.+d, 33.35.Ex, 41.85.Lc, 76.30.Rn

I. INTRODUCTION

Electron-spin-resonance (ESR) techniques have been extensively used for a study of metal clusters, mostly trimers [1–9] but some larger clusters [9–12] as well, and proved to be very powerful for obtaining the cluster geometry and electron configuration. However, all the studies up to now have been performed only for matrix-isolated clusters or clusters prepared in matrices made of, typically, frozen rare gas or hydrocarbon. A serious problem inherent in the matrix experiments is the matrix effects, that is, unknown effects given by the support. Another problem is a lack of direct measurements of the cluster size, which will limit applications of the method to simple clusters comprising only several atoms. The matrix effects normally seem to have only small influences on the hyperfine (hf) structure of the spectrum [2]. However, there may be exceptional cases; silver trimers prepared in C_6D_6 and in N_2 matrices, for example, have been reported to give hf structures that are distinctly different from each other [7,8].

This paper reports a matrix-free ESR experiment for $^6Li_3$. The method of molecular-beam magnetic resonance is employed, and practically pure Li_3 beams are prepared by the use of their deflections in an inhomogeneous magnetic field [13,14]. Thus the present results are free from those problems pointed out above. The measured spectrum permits a detailed analysis and leads to a close examination of the matrix results [1,2]. Some new difficulties in the experiment and the analysis are also described to make clear, to a certain degree, the possibilities and the limits of the matrix-free method.

II. EXPERIMENT

Figure 1 illustrates the apparatus used in this experiment. Lithium trimers were produced by coexpansion of lithium vapor (about 25 mbar) and argon (about 1.6 bar) through a 110-μm-diam conical nozzle. The cluster source consists of two separately heated sections, an oven and a narrow pipe with the nozzle at its end; the latter is screwed into the former. Enriched ^6Li of 95.63 at.% (chemical purity 99.9%) was purchased from Oak Ridge National Laboratory, Tennessee, and charged in the oven. Typical operating temperatures are about 950 °C at the oven and 1050–1100 °C at the nozzle. Stainless steel was used for the entire source, except the nozzle, which was drilled through a disk of nickel alloy (Inconel X750) and attached to the source.

The lithium clusters are size-selected with a pair of hexapole magnets [15,16], which focuses the beam of a desired size by magnetic deflections, as shown in Fig. 1. Only those clusters with electronic spins parallel to the field are focused; thus the focused beam is polarized. A homogeneous magnet and a microwave cavity for ESR are placed between the two hexapole magnets. The occurrence of ESR leads to defocusing of the clusters in the second hexapole magnet and causes a decrease in detector signal. The clusters are ionized on a tungsten hot ribbon in an oxygen atmosphere of about 2×10^{-6} Torr, and mass-analyzed with a quadrupole mass filter. No dimer or trimer ions were observed in the mass spectra; presumably all clusters will dissociate into atoms before the surface ionization takes place. A Fizeau-type velocity selector [resolution $\Delta v/v=0.25$ full width at half maximum (FWHM)] is used to eliminate high-speed atoms, which come about through velocity slips at the nozzle and can be a troublesome background in the cluster-size separation. Dimensions of the main parts of the apparatus are as in the parentheses below: distance between the source and the detector (1550 mm), lengths of the hexapole magnets A and B (160 and 180 mm, respectively), gap diameters of the hexapole magnets (5 mm each), length of the homogeneous magnet (160 mm), and gap width of the homogeneous magnet (20 mm).

Figure 2 shows a size-separation spectrum of lithium

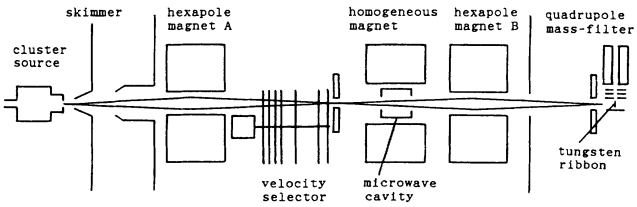

FIG. 1. Schematic diagram of the apparatus.

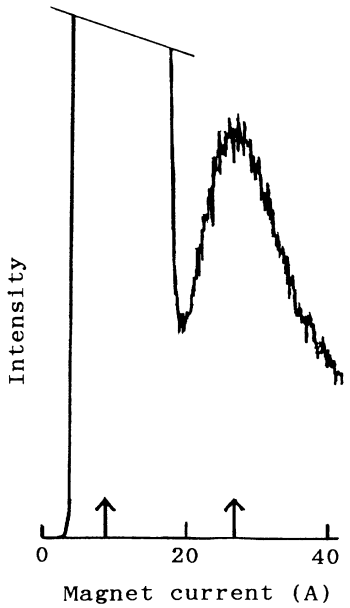

FIG. 2. Cluster-size separation by magnetic focusing. Abscissa gives currents in hexapole magnet *A*, which are about the same as those in hexapole magnet *B*. Arrows indicate positions of peaks corresponding to the atoms and the trimers.

clusters. Because the intensity of Li_5 clusters is normally much weaker than that of Li_3 when argon is the carrier gas, the selected Li_3 beam is considered to be practically pure, except that a small amount of atoms is in it. (Clusters with no unpaired electron cannot arrive at the detector because of the obstacles explained below.) In the present experiment, atomic ESR lines played an important role as marks necessary for the summation of many runs, which were repeated to get an acceptable signal-to-noise ratio. The atomic lines were also very useful for an accurate determination of the g factor for the trimers. The percentage of atoms in the selected trimer beam was adjusted to about 20% by varying the resolution of the size selection, which depends on the choice of geometric obstacles (not shown in Fig. 1) set up along the beam axis to limit the radius (both the outer and inner radii at some places) of the beam [16]. It should be mentioned that a more extensive study had been already performed for the size separation by using krypton as the carrier gas, and the size-selected clusters Li_n of $n=3$, 5, 7, 9, and 13 are clearly seen in the measured size spectrum [17].

Microwave energy of a frequency 2.453 GHz was generated by a magnetron 7090 whose output was adjusted so as to maximize a decrease in the atomic-beam intensity when atomic lines were at resonance. The ESR signal was obtained by modulating the homogeneous field at 37 Hz by the amount of 1.3 G (peak-to-peak amplitude) and measuring the synchronous change in the beam intensity with a lock-in amplifier. The homogeneous field was varied stepwise from 810 to 940 G, with an increment of 0.213 G. A single run of the ESR measurement took about 50 min, and the run was repeated 90 times. The very long acquisition time was required not because the trimer beam was weak in intensity but because it always fluctuated nervously. A higher frequency for the field modulation was not advantageous owing to a slow response of the detector.

III. RESULTS AND ANALYSIS

The measured ESR spectrum is shown in Fig. 3. The three atomic lines due to nuclear spin $I=1$ of ^6Li have an equal intensity, which corresponds to about a 5% decrease in the beam intensity. (They are cut at the half maximum and the half minimum in Fig. 3.) Other lines are much weaker, but we can clearly see seven lines located at equal intervals. They give the hf structure for $^6Li_3$. There may be many other lines arising from the spin-rotation interaction in the trimer, but most of them are not very clear. It is difficult to make a clear distinction between these minor structures and the background, whose typical variation is considered to be about one-tenth of the strongest hf line of the trimer.

The seven equally spaced lines indicate an equilateral-triangle structure of $^6Li_3$, though this is not a stable geometry, according to the Jahn-Teller theorem, for the ground electronic state of an alkali trimer. A recent spectroscopic study [18] has made it clear for Li_3 that the low-energy barrier to the pseudorotation leads to the absence of the localized vibronic states; that is, the trimer appears always pseudorotating if we see it on the time scale of $\tau \simeq 10^{-12}$ s, which is the duration for the lowest vibronic state to keep localization in one of three potential wells. Because the pseudorotation modulates the isotropic hf splittings very rapidly, the exchange narrowing is practically complete, and the three atoms in the trimer are made equivalent in ESR experiments [6,19]. We therefore interpret the present data in terms of the average hf splitting constant $\bar{a}$, which may be related to the instantaneous values as $\bar{a}=(a_1+a_2+a_3)/3$ [5,6,20,21]. We may neglect the line broadening (due to incompleteness of the exchange narrowing) and the dynamic frequency shift of the hf lines because $\tau\bar{a}/h \simeq 10^{-5}$, which means that the line broadening $\Delta\bar{a}$ will roughly be $\Delta\bar{a} \simeq 10^{-5}\bar{a}$, and the dynamic frequency shift will be much smaller than $\Delta\bar{a}/h$ [19,21].

The spin Hamiltonian in a magnetic field $\mathbf{B}$ may be written as a sum of the electronic Zeeman energy, the hf interaction, and the spin-rotation interaction:

$$H=H_{\mathrm{EZ}}+H_{\mathrm{hf}}+H_{\mathrm{SR}}$$
$$=g\beta\mathbf{B}\cdot\mathbf{S}+\bar{a}\mathbf{S}\cdot\mathbf{T}+\gamma\mathbf{S}\cdot\mathbf{N}\ , \tag{1}$$

where β is the Bohr magneton, $\mathbf{T}$ is the total nuclear spin angular momentum, $\mathbf{T}=\mathbf{I}_1+\mathbf{I}_2+\mathbf{I}_3$, and $\mathbf{N}$ is the angular momentum of the molecular rotation. The nuclear Zeeman term $H_{\mathrm{NZ}}=-g_n\beta_n\mathbf{B}\cdot\mathbf{T}$ is omitted here to make it clear that its effects are negligible or much smaller than the experimental errors in this work. A problem in our Hamiltonian is that we have very restricted knowledge of the spin-rotation term H_{SR}; however, we carry on our analysis by temporarily assuming that

$$\gamma^2 \ll \bar{a}^2 \tag{2}$$

and solving the eigenvalue problem by perturbation theory. The above assumption is discussed in detail in

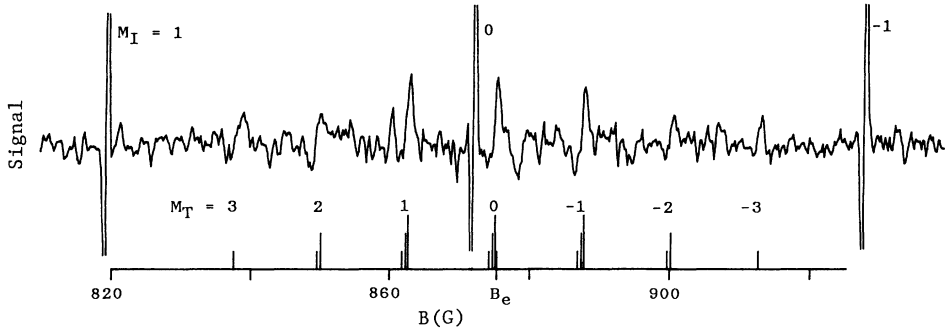

FIG. 3. ESR spectrum of pseudorotating $^6Li_3$. Three atomic lines are cut at the half maximum and the half minimum. $B_e = 875.3$ G is the resonance field of a free electron. Stick diagram shows the calculated hf transitions for the trimer; the stick length is proportional to the degree of degeneracy: $T=2$ is doubly and $T=1$ is triply degenerate.

the Appendix. Then, the energy interval $h\nu$ between Zeeman levels at resonance is given as

$$h\nu = g\beta B + \bar{a}M_T + (\bar{a}^2/2g\beta B)[T(T+1) - M_T^2] + \gamma M_N \ . \tag{3}$$

The last term in this equation will give a symmetrical distribution of lines centering about the strongest one at $M_N = 0$, and therefore may utterly be neglected if the central line in each hf component is clearly identified in the measured spectrum. In addition, the lines $M_N \neq 0$ will be considerably weaker than the $M_N = 0$, because the coupling constant γ in H_{SR} depends in general on the rotational quantum numbers N and K [22], and this will modify the line positions so as to smooth out the structures due to H_{SR}. Thus, we set $M_N = 0$ in Eq. (3) and try to clarify the hf structure and the g factor of the measured spectrum.

The final problem to be settled for an accurate analysis is the second-order hf effects. It will make this problem clearer to see first the final results of calculations that are shown in Fig. 3 in the form of a stick diagram. In Fig. 3, a substantial shift of the atomic line $M_I = 0$ from B_e (resonance field of a free electron) is due to the second-order hf term, while corresponding shifts of the trimer's lines $M_T = 0$ are greatly reduced because $\bar{a}^2 \ll a_{atom}^2$, where

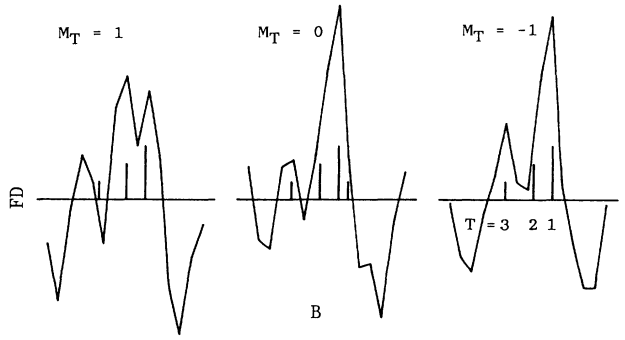

FIG. 4. Second-derivative analysis for $M_T = 1$, 0, and -1. The finite difference (FD) of the original spectrum is plotted. Intervals of the data points are 0.213 G. The stick diagram is the same as in Fig. 3.

a_{atom} is the hf constant for a free ^6Li atom. However, it is clear from the apparent asymmetry of the first-order components $M_T = -1$ to 1 that the second-order effects must be carefully taken into account. The second-derivative curve (the finite difference of the measured spectrum) was used for a closer analysis of the lines $M_T = -2$ to 2, and it has been found that these lines actually consist of two components, the $T=3$ component, and the rest. Figure 4 illustrates this analysis for $M_T = 1$, 0, and -1. The separation between $T=3$ and $T=0$–2 is clear. However, the line ($M_T = 1$, $T=3$) is either missing or exceptionally disagreeing with the calculated result though all other lines are much better reproduced by the same calculation. Only this particular line was omitted, and all other 11 lines (six lines with $T=3$ and five lines with $T \neq 3$) were used in the χ^2 minimization for the parameter fitting. Positions of the unresolved lines were assumed to show the weighted average of the second-order hf components involved.

The best-fit parameters with their estimated errors are $g = 2.002\,36 \pm 0.000\,07$ and $\bar{a}/g_e\beta = 12.52 \pm 0.02$ G, where $g_e = 2.002\,32$ is the g factor of a free electron. The isotropic spin population $\rho = a/a_{atom}$ is given to be $\bar{\rho} = \bar{a}/a_{atom} = 0.231$. The error in the g factor is mainly due to the uncertainty in the relative positions of the trimer's lines with respect to the atomic lines, while the error in $\bar{a}/g_e\beta$ is dominated by the uncertainty in the distances between the trimer's lines.

The measured g factor is nearly equal to g_e. This will be confirmed by estimating [19] the g shift $\Delta g = g - g_e$ as

$$\Delta g \simeq -(1 - 3\bar{\rho})\lambda/(E_1 - E_0) \ , \tag{4}$$

where λ is the spin-orbit coupling constant for the $2p$ orbital of the atom, $E_1 - E_0$ is the electronic excitation energy to the lowest excited state of the trimer, and the factor $1 - 3\bar{\rho}$ means a fractional p character of the unpaired electron. The small nuclear charge of lithium gives a very low λ of 0.2 cm^{-1} (=0.03 meV) [23]. From an estimation of $E_1 - E_0 \simeq 0.7$ eV [24], we obtain $\Delta g \simeq -1 \times 10^{-5}$. The experimental result above is consistent with the estimation, and this fact indirectly justifies the assumed inequality (2), under which we neglected the second-order effects of H_{SR}. In fact, the

small $|\Delta g|$ implies a weak spin-rotation interaction, as explained in the Appendix.

IV. COMPARISONS AND FINAL REMARKS

In Table I, the measured g, $\bar{a}$, and $\bar{\rho}$ for the free trimers are compared with previous results for the matrix-isolated trimers [1,2], and some typical data for the atoms [1,2,15] are also listed for comparison of the matrix effects. Our primary interest here is in the variation of Δg and $(\rho-\rho_f)/\rho_f$, where ρ_f means the isotropic spin population for a free Li_3 or Li atom. From these comparisons we may say the following: (1) the matrix effects for the trimers are about the same in magnitude as those for the atoms, but one cannot predict the former from a knowledge of the latter straightforwardly; (2) $|\rho-\rho_f|/\rho_f$ is small, or about 0.03 or less for all data given here; (3) Δg depends considerably on the matrix material, and the matrix experiments do not seem to give any useful information on Δg for free trimers or atoms. The above comparisons strongly support the idea that the hf structures obtained in the matrix experiments are basically independent of the matrix material used, and give reliable information on the geometry and the electronic structure of free metal clusters. Garland and Lindsay [1] have found that a total isotropic spin population ($3\bar{\rho}$) in Li_3 is remarkably smaller than unity, though it is much closer to unity in Na_3 and K_3 [25]. This is confirmed by the present experiment. It should be remarked that the matrix effects often depend not only on the matrix material but also on the matrix site on which clusters rest. Three matrix sites are reported for ^{7}Li atoms in adamantane matrices [2], and a weak signal from a second matrix site is observed for $^6Li_3$ in argon matrices [26].

If the second-order hf splittings are negligible, the relative intensities of the hf transitions will be in the ratio 1:3:6:7:6:3:1. The trimers in argon matrices indeed give this ratio at the resonance field of about 3300 G [1]. On the other hand, the intensity pattern in Fig. 3 is 1.2:1.4:2.4:2.4:2.3:1.1:1.0. It seems that closely located hf lines did not necessarily give an enhanced signal in the present experiment. This will be, at least partly, due to the fact that the field modulation used in the experiment was too large in amplitude as compared with the narrow linewidths characteristic of free molecules. In this situation, a severe distortion of the sine-wave signal will be caused by the closely located lines, and level down the signal from expected magnitudes. This effect will be small for $M_T=\pm 3$, which consists of only one major line ($T=3$, $M_N=0$) and minor lines $M_N\neq 0$.

It will be helpful to summarize how much the choice of ^{6}Li affects this experiment: (1) the small mass makes the magnetic deflection easy; (2) the small nuclear spin and the low $\bar{a}$ value (about 1/3.5 that of ^{7}Li) give a simple and clear hf structure; (3) the very small λ (about 1/60 that of Na) reduces the effects of H_{SR} to minor disturbances. The disadvantage of using lithium is that the production of intense and cold cluster beams is difficult because of the high temperatures required. Larger lithium clusters will be studied by the molecular-beam ESR as the method of the cluster production is improved.

APPENDIX

Magnitude of $H_{SR}=\gamma\mathbf{S}\cdot\mathbf{N}$ in Li_3

The spin-rotation coupling constant γ may be divided as $\gamma=\gamma_1+\gamma_2$. Here γ_1 is due to the direct interaction of the spin with the magnetic field of molecular rotation, while γ_2 arises from the combined effect in which molecular rotation excites orbital angular momentum of the electron, and couples to the spin through spin-orbit interaction [27,28]. The second effect, which normally dominates, has a close relation [28] to the cause of the g shift and may be given as

$$\gamma_2\simeq -2B'\Delta g \ , \tag{A1}$$

where $B'=(2B+A)/3$ denotes the average rotational constant obtained from $B=0.681$ cm^{-1} and $A=0.333$ cm^{-1} [29]. Using Eq. (4) to estimate Δg, we obtain $\gamma_2/g_e\beta\approx 0.2$ G. The first effect giving γ_1 is usually unimportant, but should also be evaluated in case of small γ_2. We consider the magnetic field (in laboratory coordinates) $\mathbf{b}(\mathbf{r})$ produced by the rotation of effective nuclear charges, and average the field with respect to the position $\mathbf{r}$ of the unpaired electron. The expectation value $\langle\mathbf{b}\rangle$ may be written as

$$\langle\mathbf{b}\rangle=(Z'e/c)\sum_i(\boldsymbol{\omega}\times\mathbf{R}_i)\times\langle(\mathbf{r}-\mathbf{R}_i)/|\mathbf{r}-\mathbf{R}_i|^3\rangle \ , \tag{A2}$$

where $Z'e$ is the effective nuclear charge, $\boldsymbol{\omega}$ the angular velocity of the rotation, and $\mathbf{R}_i$ the position of the ith nucleus; positions are measured from the center of mass.

TABLE I. ESR parameters for the matrix-free and the matrix-isolated Li_3 clusters, along with similar comparisons for the atoms. $\bar{a}=a$ and $\bar{\rho}=\rho$ for the atoms.

Species	Matrix	g factor	$\bar{a}/g_e\beta$ (G)	$\bar{\rho}$	Ref.
$^6Li_3$	free	2.002 36	12.52	0.231	this work
$^6Li_3$	argon	2.002 82	12.21	0.225	1
$^7Li_3$	adamantane	2.0010	33.1	0.231[a]	2
^{6}Li	free	2.002 31	54.29	1	15
^{6}Li	argon	2.000 11	56.06	1.03	1
^{7}Li (I)[b]	adamantane	2.0023	139.8	0.975[a]	2

[a] $a/g_e\beta$ for a free ^{7}Li atom is 143.36 G from Ref. [15].
[b] Matrix site I.

The quantity in brackets above may be evaluated by using Slator orbitals ($Z'=1.3$) on each atom. We mix $2s$ and $2p$ orbitals according to the measured $\bar{\rho}$, since without this mixing the expectation value averages to zero. The trimer is regarded as an equilateral triangle with side length of 2.89 Å [29], and the p orbital is assumed to be in the direction toward the center of mass. The field $\langle b_z \rangle$, after an average over three independent rotations, gives γ_1 as $\gamma_1/g_e\beta=\langle b_z \rangle/M_N \approx 0.1$ G.

Thus γ is approximately found to be $\gamma/g_e\beta \approx 0.3$ G, which is far smaller than $\bar{a}/g_e\beta$. We will complete the discussion by estimating the most probable value N_{MP} of the rotational quantum number N, since γ must actually satisfy $\gamma^2 N_{\mathrm{MP}}^2 \lesssim \bar{a}^2$ for justification of our treatment. The intensities of the seven hf lines in Fig. 3 correspond to about 0.4–1 % decreases in the beam intensity, and this means that about one-tenth of the trimers in the beam are effectively contributing to the signal at the peaks. If only the lines $M_N=0$ contribute to the signal, the experimental yield may be understood as $\frac{1}{10} \simeq 1/(2N_{\mathrm{MP}}+1)$, or $N_{\mathrm{MP}} \simeq 5$. This may be an underestimate if $\gamma/g_e\beta \approx 0.3$ G is correct, since contributions of $M_N=\pm 1$ are totally neglected. However, $N_{\mathrm{MP}} \simeq 5$ will become realistic if γ is, in fact, considerably larger than our estimate; therefore $\gamma^2 N_{\mathrm{MP}}^2$ will remain small enough to satisfy the above condition.

[1] D. A. Garland and D. M. Lindsay, J. Chem. Phys. **78**, 2813 (1983).

[2] J. A. Howard, R. Sutcliffe, and B. Mile, Chem. Phys. Lett. **112**, 84 (1984).

[3] D. M. Lindsay, D. R. Herschbach, and A. L. Kwiram, Mol. Phys. **32**, 1199 (1976).

[4] D. M. Lindsay, D. R. Herschbach, and A. L. Kwiram, Mol. Phys. **39**, 529 (1980).

[5] G. A. Thompson and D. M. Lindsay, J. Chem. Phys. **74**, 959 (1981).

[6] G. A. Thompson, F. Tischler, D. Garland, and D. M. Lindsay, Surf. Sci. **106**, 408 (1981).

[7] J. A. Howard, K. F. Preston, and B. Mile, J. Am. Chem. Soc. **103**, 6226 (1981).

[8] K. Kernisant, G. A. Thompson, and D. M. Lindsay, J. Chem. Phys. **82**, 4739 (1985).

[9] L. B. Knight, Jr., R. W. Woodward, R. J. Van Zee, and W. Weltner, Jr., J. Chem. Phys. **79**, 5820 (1983).

[10] G. A. Thompson, F. Tischler, and D. M. Lindsay, J. Chem. Phys. **78**, 5946 (1983).

[11] J. A. Howard, K. F. Preston, R. Sutcliffe, and B. Mile, J. Phys. Chem. **87**, 536 (1983).

[12] J. A. Howard, R. Sutcliffe, J. S. Tse, and B. Mile, Chem. Phys. Lett. **94**, 561 (1983).

[13] W. D. Knight, R. Monot, E. R. Dietz, and A. R. George, Phys. Rev. Lett. **40**, 1324 (1978).

[14] W. D. Knight, Helv. Phys. Acta **56**, 521 (1983).

[15] P. Kush and V. W. Hughes, in *Atoms III–Molecules I*, edited by S. Flügge, Handbuch der Physik Vol. 37, Part 1 (Springer, Berlin, 1959).

[16] N. Hishinuma and O. Sueoka, Chem. Phys. Lett. **98**, 414 (1983).

[17] N. Hishinuma and C. Amano, At. Collision Res. Jpn. **16**, 152 (1990).

[18] Ph. Dugourd, J. Chevaleyre, M. Broyer, J. P. Wolf, and L. Wöste, Chem. Phys. Lett. **175**, 555 (1990).

[19] C. P. Slichter, *Principles of Magnetic Resonance* (Harper and Row, New York, 1964).

[20] D. M. Lindsay and G. A. Thompson, J. Chem. Phys. **77**, 1114 (1982).

[21] G. K. Fraenkel, J. Chem. Phys. **42**, 4275 (1965).

[22] C. C. Lin, Phys. Rev. **116**, 903 (1959).

[23] G. F. Kirkbright and M. Sargent, *Atomic Absorption and Fluorescence Spectroscopy* (Academic, London, 1974).

[24] F. Cocchini, T. H. Upton, and W. Andreoni, J. Chem. Phys. **88**, 6068 (1988).

[25] $3\bar{\rho}=0.87$ for Na_3 and 0.89 for K_3 (see Refs. [3], [5], [6], [20]).

[26] The second matrix site has $g=2.003\,54$ and $\bar{a}/g_e\beta=12.12$ G, as given in Ref. [1].

[27] J. H. Van Vleck, Rev. Mod. Phys. **23**, 213 (1951).

[28] R. F. Curl, Jr., Mol. Phys. **9**, 585 (1965).

[29] J. Blanc, M. Broyer, J. Chevaleyre, Ph. Dugourd, H. Köhling, P. Labastie, M. Ulbricht, J. P. Wolf, and L. Wöste, Z. Phys. **D19**, 7 (1991).